JOURNAL OF SOLID STATE CHEMISTRY 56, 343–354 (1985)

Magnetic Order in AVX_3 (A = Rb, Cs, $(CD_3)_4$ N; X = Cl, Br, I): A Neutron Diffraction Study

ANDREAS HAUSER,* URS FALK†, PETER FISCHER,† AND HANS U. GÜDEL*,‡

†*Labor für Neutronenstreuung ETHZ CH-5303 Würenlingen, Switzerland, and* **Institut für anorganische Chemie der Universität Bern Freiestrasse 3, CH-3000 Bern 9, Switzerland*

Received April 5, 1984; in revised form September 7, 1984

AVX_3 (A = Rb, Cs, $(CD_3)_4$ N; X = Cl, Br, I) crystallize in the hexagonal system, space group $P6_3/mmc$, with chains of face-sharing VX_6 octahedra along the c-axis. This leads to a pronounced one-dimensional character of their magnetic properties with a strong antiferromagnetic exchange interaction J between nearest neighbor V^{2+} ions along these chains. All compounds except $[(CD_3)_4N]VCl_3$ order three-dimensionally with ordering temperatures T_c between 13 and 32 K. In the ordered phase the magnetic moments, μ, lie in the basal plane in a triangular arrangement typical for antiferromagnetic interchain interaction J'.

1. Introduction

Among the large class of compounds with stoichiometry AMX_3, where A = alkali metal, M = 3d transition metal, and X = halogen, those containing V^{2+} have received relatively little attention until quite recently. At room temperature $CsVX_3$ (X = Cl, Br, I) as well as $RbVCl_3$ and $RbVBr_3$ are reported to crystallize in the hexagonal space group $P6_3/mmc$ (*1, 2*) with Z = 2. Crystal structures have been determined for $CsVCl_3$ by single-crystal X-ray diffraction (*3*) and for $CsVI_3$ and $RbVI_3$ by powder neutron diffraction (*4*). They crystallize in the well-known $CsNiCl_3$ structure with chains of face-sharing MX_6-octahedra running parallel to the c-axis, separated by alkali ions.

The magnetic susceptibilities of $CsVX_3$ reported in the temperature range 4–800 K exhibit broad maxima typical for one-dimensional (1D) antiferromagnets with large intrachain exchange couplings (*5*). No transition to 3D magnetic order could be observed by this technique so far. However, the *ac*-susceptibility of a single crystal of $CsVBr_3$ with $h \| c$ shows an anomalous behavior around 28 K (*6*).

By using neutron diffraction Zandbergen (*4*) found $CsVI_3$ and $RbVI_3$ to order antiferromagnetically at 32(1) and 25(1) K, respectively. The magnetic structures were found to be triangular with the magnetic moments in the basal plane. Recently Hirakawa *et al.* (*7*) and us (*8*) showed that $CsVCl_3$ orders in the same magnetic structure below 13.3 K. Hirakawa found an unexpected decrease in the ordered magnetic moment below 4.2 K and suggested that this might be due to spin

‡ To whom correspondence should be addressed.

0022-4596/85 $3.00

pairing at low temperatures as proposed by Anderson (*9*). Steiner *et al.* (*10*) studied the 1D spin correlation in $CsVCl_3$ up to room temperature by quasielastic neutron scattering.

Single-crystal optical spectra of $CsVX_3$ show clear evidence of strong intrachain spin correlations (*11*). In $CsVBr_3$ and $RbVBr_3$ the intensity of a magnon sideband in the absorption spectrum was found to be a measure of the 3D magnetic order. Zeeman experiments on the $^4A_{2g} \rightarrow {}^2T_{2g}$ transition show that no-phonon optical transitions could be interpreted in terms of the triangular spin structure (*12*).

In this paper we report the high- and low-temperature nuclear structures, the transitions to 3D magnetic order, and the magnetic structures of $RbVCl_3$, $RbVBr_3$, $CsVCl_3$, $CsVBr_3$, and $CsVI_3$ and the nuclear structure of $[(CD_3)_4N]$ VCl_3 (TMVC). The 1D vs 3D character of the various compounds as well as the observed reduction in the ordered magnetic moment will be discussed.

2. Experimental

2.1. Preparation of Compounds

Starting materials for the synthesis of the AVX_3 compounds (A = Rb, Cs; X = Cl, Br, I) are the binary alkali halides AX and V^{2+} halides VX_2. Suprapure AX compounds (Merck) and VI_2 (Cerac) were used. VCl_2 and VBr_2 were synthesized according to the reaction $2VX_3 + V \rightarrow 3VX_2$ as suggested by Smith (*13*). Stoichiometric mixtures of vanadium metal (Fluka 99.7%) and the corresponding trihalide VX_3 (Cerac 99.0%) were sealed in evacuated quartz ampoules and slowly heated to 850°C. After a few days, when the reaction was completed, the products were sublimed in a temperature gradient of 150°C along the ampoules for purification, the temperature of the hot end being kept at 1050°C for VCl_2 and 900°C for VBr_2. Light-green hexagonal VCl_2 and reddish brown VBr_2 crystals could be collected at the cold end of the ampoules. The AVX_3 compounds $RbVCl_3$, $RbVBr_3$, $CsVCl_3$, $CsVBr_3$, and $CsVI_3$ were prepared by fusing equimolar mixtures of the binary compounds in evacuated quartz ampoules at 750°C for 3 days (*3*, *14*). In all cases the products consisted of very fine long needles which could be detected with a microscope. The chlorides are dark green, the bromides brown, and the iodide red. These products as well as the VX_2 compounds are hygroscopic and air sensitive and must be handled in a dry box.

AVX_3 single crystals were grown by the Bridgman method at a rate of 1.8 mm/h, the temperature of the furnace was chosen 50°C above the melting point of the specific compound (m.p. $CsVCl_3$, 1085°C (*3*); $CsVBr_3$, 1065°C (*3*); $CsVI_3$, 900°C (*14*); $RbVCl_3$, 1020°C (*2*); $RbVBr_3$, 990°C (*16*)). The crystals cleave easily along the hexagonal c-axis, but not at all perpendicular to it. Owing to this pronounced structural anisotropy single crystals with a mosaic structure smaller than 1° in the c-direction were rarely obtained.

$[(CD_3)_4$ N] VCl_3 (TMVC) was precipitated from a solution of VCl_2 in ethanol containing 10% HCl by adding an equimolar amount of a saturated ethanolic solution of $[(CD_3)_4$ N]Cl (*15*). The light-brown precipitate was filtered, washed with ether/ethanol (1 : 1), and dried under vacuum. The VCl_2 solution was prepared electrolytically (*16*). All manipulations were performed under an N_2 atmosphere because the V^{2+} solution is unstable in air. The product is very hygroscopic and air sensitive and must be handled in a dry box. Attempts at growing single crystals from solution were not successful.

2.2. Neutron Diffraction Experiments

All neutron diffraction measurements were done at the reactor Saphir in Würenlingen. The wavelength was fixed at

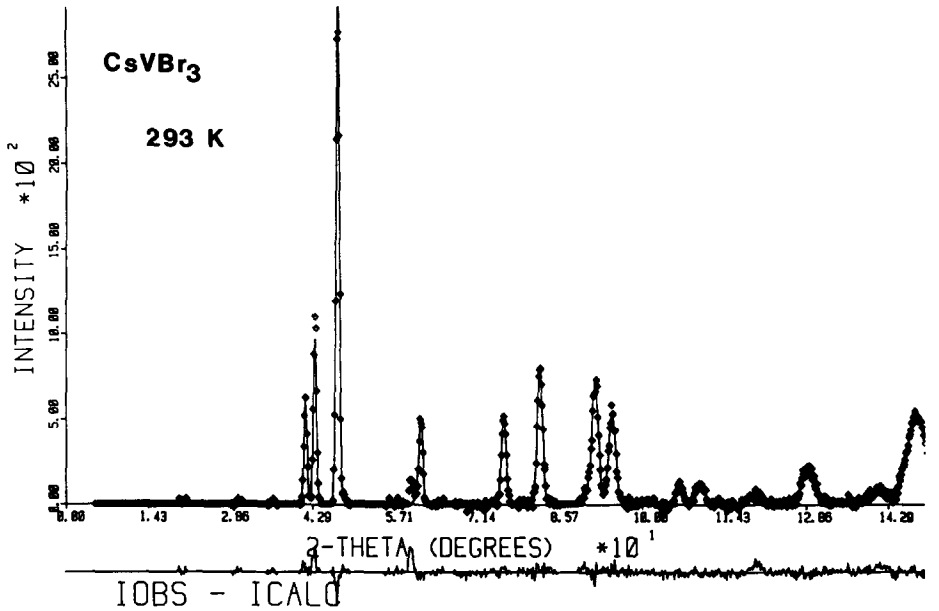

FIG. 1. Neutron powder diffraction profile at 293 K of $CsVBr_3$. $\lambda = 2.34$ Å.

2.34 Å. Two-axis spectrometers were used for the powder and single-crystal measurements. The powder data were corrected for absorption, and the profile program of Rietveld (*17*) was used for the refinement of both nuclear and magnetic structures. The integrated R_I and weighted profile R_{wp} values used in the least-squares fitting procedure are those defined in Ref. (*17*). The coherent scattering lengths were taken from Ref. (*18*) and the magnetic form factors for V^{2+} from Watson and Freeman (*19*).

Temperatures down to 6 K for the powder measurements were achieved with a closed-cycle refrigerator (Cryogenics) and a helium cold finger cryostat, and down to 1.5 K for some of the single-crystal measurements with a Thor helium gas flow cryostat.

3. Nuclear Structures

3.1. $CsVCl_3$, $CsVBr_3$, and $RbVCl_3$

Figure 1 shows, as an illustration, the room-temperature neutron powder diffraction profile of $CsVBr_3$. The 293 and 4.2 K profiles of all the three compounds can be interpreted with the nuclear structure of space group $P6_3/mmc$ and the following atomic positions in the unit cell:

V	2(*a*)	(0 0 0); (0 0 $\frac{1}{2}$)
A	2(*d*)	$\pm(\frac{1}{3}\ \frac{2}{3}\ \frac{3}{4})$
X	6(*h*)	$\pm(x\ 2x\ \frac{1}{4})$; $\pm(2\bar{x}\ \bar{x}\ \frac{1}{4})$; $\pm(x\ \bar{x}\ \frac{1}{4})$

There is only one adjustable positional parameter x. All the structural parameters obtained from the least-squares refinements are collected in Table I. The unit cell dimensions at room temperature are in good agreement with those determined by powder X-ray diffraction (*1–3*). The same is true for the positional parameter x in $CsVCl_3$ (*3*). In all the compounds, both at 293 and 4.2 K, the V^{2+} coordination corresponds to a slightly trigonally elongated VX_6 octahedron. The shrinking of the unit cell between 293 and 4.2 K is of the order $5–10 \times 10^{-2}$ Å and more or less isotropic.

TABLE I

UNIT CELL DIMENSIONS a AND c, POSITIONAL PARAMETER x, DISTANCE V–X, ANGLE α BETWEEN c AXIS AND V–X, OVERALL DEBYE–WALLER FACTOR B, AND R FACTORS OF REFINEMENT

Compound	T (K)	a [Å]	c [Å]	x	V–X [Å]	α	B(T) [Å^2]	R_{wp}^{nucl}	R_I^{nucl}
$CsVCl_3$	293	7.237(1)	6.026(1)	0.157	2.48	52.64	1.65	0.11	0.059
$CsVBr_3$	293	7.570(1)	6.320(1)	0.160	2.63	53.00	1.67	0.18	0.087
$CsVI_3$[a]	293	8.124(1)	6.774(1)	0.169	2.92	54.54	2.9	0.13	0.044
$RbVCl_3$	293	7.051(1)	5.985(1)	0.164	2.50	53.20	1.9	0.13	0.082
$RbVBr_3$	293	7.408(1)	6.280(1)	0.166	2.65	53.66	2.18	0.14	0.059
$CsVCl_3$	5	7.187(1)	5.989(1)	0.159	2.48	52.81	—	0.12	0.072
$CsVBr_3$	6.5	7.504(1)	6.262(1)	0.160	2.60	52.96	—	0.10	0.058
$CsVI_3$[a]	1.2	8.062(1)	6.704(1)	0.173	2.94	55.31	0.1	0.14	0.070
$RbVCl_3$	4.2	6.988(1)	5.930(1)	0.164	2.47	53.14	—	0.09	0.027
$RbVI_3$[a]	293	13.863(2)	6.807(1)				4.5	0.13	0.09
TMVC	293	9.120(4)	6.248(3)					0.20	0.09
TMVC	1.7	9.027(3)	6.232(3)	Different space group			—	0.11	0.08
$RbVI_3$[a]	1.2	13.750(2)	6.761(2)				1.5	0.17	0.13
$RbVBr_3$	4.2	12.739(2)	6.247(1)				—	0.14	0.08

[a] Ref. (*4*).

3.2. *$RbVBr_3$*

$RbVBr_3$ shows a different behavior. At room temperature it has the same nuclear structure as the compounds mentioned in Section 3.1. (room-temperature parameters for $RbVBr_3$, see Table I), but upon lowering the temperature a new, weak reflection appears at $2\theta = 45.8°$ below 98 ± 2 K, indicating a structural phase transition. In Fig. 2 the 293 and 33 K diffraction profiles of $RbVBr_3$ and the temperature dependence of the $2\theta = 45.8°$ reflection are shown. From the temperature dependence we conclude that the phase transition is of second order. The new reflection in the low-temperature (LT) phase can be indexed as (1 0 2) by enlarging the high-temperature unit cell to $\sqrt{3}a$, $\sqrt{3}a$, c, containing three VBr_3 chains. The (1 0 2) is the only fully resolved new reflection in the LT powder diagram. The (1 2 3), (3 1 3), and (1 0 4) are superimposed by the very intense reflections (6 0 0), (2 2 3), and (0 0 4), respectively. Possible space groups for the LT phase are $P6_3cm$ and $P\bar{3}c1$. Table II lists the results of the least-squares refinements in the two space groups. No distinction is possible on the basis of the present data. Evidence for a

TABLE II

STRUCTURAL PARAMETERS FOR THE LOW-TEMPERATURE PHASE OF $RbVBr_3$ (33 K)

a = 12.746(2) Å c = 6.248(2) Å
B = 0.61(9) Å^2

$P6_3cm$	R_{wp}^{nucl} = 0.14		R_I^{nucl} = 0.073	Wyckoff positions
V	0	0	0	(a)
	$\frac{1}{3}$	$\frac{2}{3}$	0.055(2)	(b)
Rb	0.329(4)	0.329(4)	0.258(3)	(d)
Br	0.164(4)	0	$\frac{1}{4}$	(c)
Br	0.503(3)	0.163(2)	0.305(2)	(d)
$P\bar{3}c1$	R_{wp}^{nucl} = 0.14		R_I^{nucl} = 0.079	
V	0	0	0	(b)
	$\frac{1}{3}$	$\frac{2}{3}$	0	(d)
Rb	0.327(3)	0.327(3)	$\frac{1}{4}$	(f)
Br	0.168(5)	0	$\frac{1}{4}$	(f)
Br	0.505(3)	0.168(2)	0.216(2)	(g)

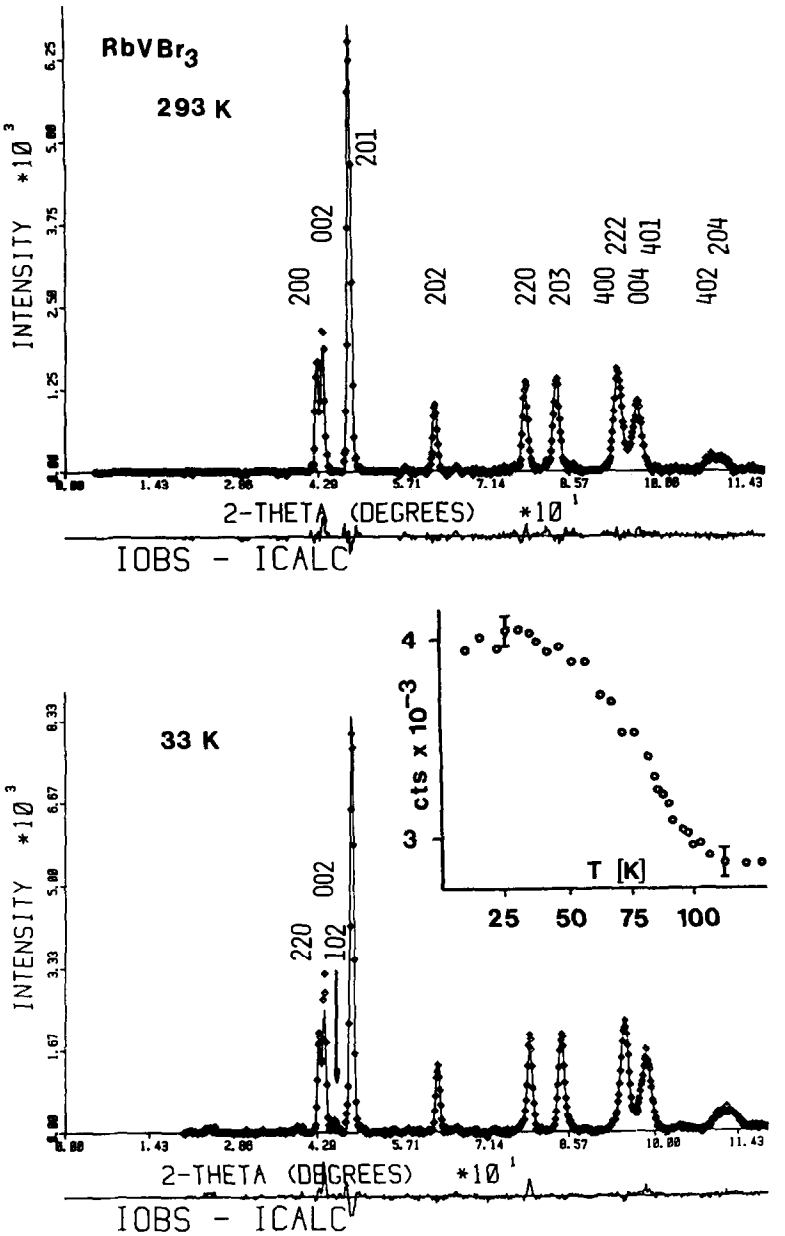

FIG. 2. Neutron powder diffraction profiles of $RbVBr_3$ at 293 and 33 K. For the 33 K diagram indices refer to the enlarged nuclear unit cell. Inset: temperature dependence of the low-temperature phase (1 0 2) reflection. $\lambda = 2.34$ Å.

similar structure even at room temperature in $RbVI_3$ was found by Zandbergen (*4*). The deviation from the space group of higher symmetry $P6_3/mmc$ can be interpreted in terms of a model in which the VBr_3 chains as a whole without deformation are displaced against each other along the *c*-axis. In any case the shifts are small.

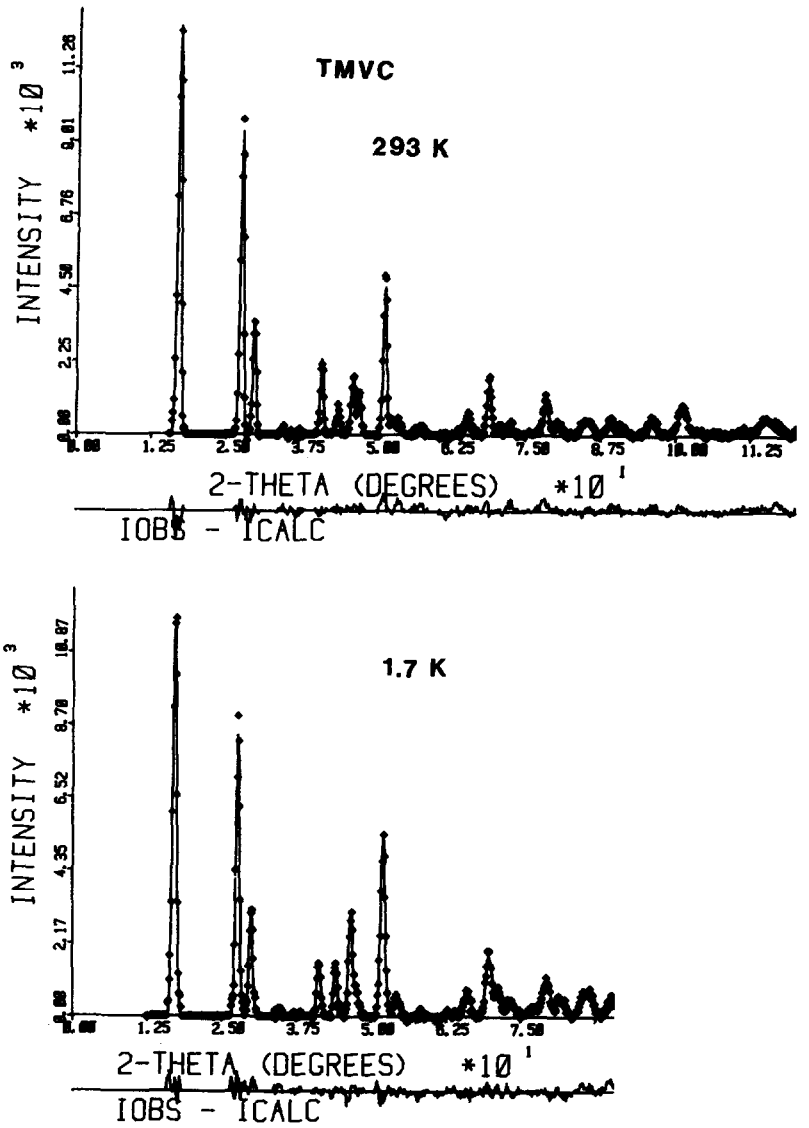

FIG. 3. Neutron powder diffraction profiles of TMVC at 293 and 1.7 K. $\lambda = 2.34$ Å.

3.3. $[(CD_3)\ N]\ VCl_3$ (TMVC)

Owing to the complex structure of the tetramethylammonium ion the nuclear structure of TMVC is somewhat more complicated than the nuclear structure of the other AVX_3 compounds investigated. Nevertheless TMVC still crystallizes in the hexagonal crystal system and the chains of face-sharing VCl_6 octahedra are retained. At 40 K a second-order phase transition occurs corresponding mainly to a reorientation of the tetramethylammonium ion.

TMVC at 1.7 K. Figure 3a shows the 1.7 K neutron powder diffraction profile of TMVC. The lattice constants were found to be $a = 9.027(3)$ Å and $c = 6.232(3)$ Å. At this temperature TMVC appears to be iso-

TABLE III

STRUCTURAL PARAMETERS OF TMVC AT 293 AND 1.7 K AND SOME SELECTED BOND LENGTHS

		293 K $P6_3/m$ $a = 9.120(4)$ Å $c = 6.284(3)$ Å $R_{wp}^{nucl} = 0.20$ $R_I^{nucl} = 0.09$				1.7 K $P6_3$ $a = 9.027(3)$ Å $c = 6.232(3)$ Å $R_{wp}^{nucl} = 0.11$ $R_I^{nucl} = 0.08$			
Atom	Occup. number	x	y	z	Wyckoff position	x	y	z	Wyckoff position
V	1	0.	0.	0.	(b)	0.	0.	0.	(a)
N	1	$\frac{1}{3}$	$\frac{2}{3}$	$\frac{1}{4}$	(c)	$\frac{1}{3}$	$\frac{2}{3}$	$\frac{1}{4}$	(b)
Cl	1	0.143(2)	0.227(1)	$\frac{3}{4}$	(h)	0.158(4)	0.244(3)	0.80(2)	(c)
C(1)	$\frac{1}{2}$	$\frac{1}{3}$	$\frac{2}{3}$	−0.013(1)	(f)	$\frac{1}{3}$	$\frac{2}{3}$	−0.01(2)	(b)
C(2)	$\frac{1}{2}$	0.140(2)	0.633(3)	0.292(6)	(i)	0.15(1)	0.61(1)	0.31(2)	(c)
D(1)	$\frac{1}{2}$	0.457(1)	0.725(4)	−0.057(3)	(i)	0.409(7)	0.619(6)	−0.01(2)	(c)
D(2)	$\frac{1}{2}$	0.067(4)	0.533(5)	0.418	(i)	0.16(1)	0.62(1)	0.50(2)	(c)
D(3)	$\frac{1}{2}$	0.089(4)	0.492(3)	0.312(2)	(i)	0.071(9)	0.481(9)	0.31(1)	(c)
D(4)	$\frac{1}{2}$	0.203(4)	0.719(4)	0.398(5)	(i)	0.131(7)	0.719(6)	0.20(1)	(c)
V –Cl		2.40(1) Å				2.23(7) Å			
V –V		3.14(1)				3.12(1)			
N –C(1)		1.65(1)				1.63(1)			
N –C(2)		1.65(2)				1.51(3)			
C(1)–D(1)		1.01(1)				0.97(7)			
C(2)–D(2)		1.14(4)				1.19(15)			
C(2)–D(3)		1.14(4)				1.05(10)			
C(2)–D(4)		0.97(4)				1.26(14)			

structural to $[(CH_3)_4\ N]\ NiBr_3$ (*20*) with space group $P6_3$, which leads to a systematic absence of (0 0 l) reflections with $l = 2n + 1$. The V^{2+} ions were taken at (0, 0, 0) and (0, 0, $\frac{1}{2}$). Because of their small scattering length for neutrons they do not define the origin well enough, therefore the z-coordinate of the nitrogen atom was fixed at $z = \frac{1}{4}$. Initial values for structure refinements of the chlorine and carbon atoms were taken from $[(CH_3)N]\ NiBr_3$, and the positions of the deuterium atoms were chosen according to the bond angles and bond lengths appropriate for $(CD_3)_4N^+$ according to the Handbook of Chemistry and Physics (*21*). For N–C and C–D distances soft and boundary conditions (*22*) were considered, but releasing these restrictions did not lead to significant changes in atomic positions. In Table III the results of the successive least-squares refinements with the Rietveld program are listed. The $[(CD_3)_4\ N]^+$ groups define a directional sense to the structure, in that the inverted umbrellas formed by three of the four CD_3 groups point in the same direction for all $[(CD_3)_4\ N]^+$ ions. Table III includes some relevant bond lengths.

TMVC at 298 K. The second-order phase transition at 40(10) K can be understood as the loss of directional sense imposed by the $[(CD_3)_4\ N]^+$ ions at low temperature. The high-temperature structure is still hexagonal with $a = 9.120(4)$ Å and $c = 6.284\ (3)$ Å, and it can be described by the space group $P6_3/m$, which is the same as for $[(CH_3)_4\ N]\ MnCl_3$ (*23*), with the linear chains of vanadium atoms bridged by three chlorine atoms still intact and statistically disordered $[(CD_3)_4\ N]^+$ ions.

4. Magnetic Order

All the compounds investigated except TMVC show additional reflections at small

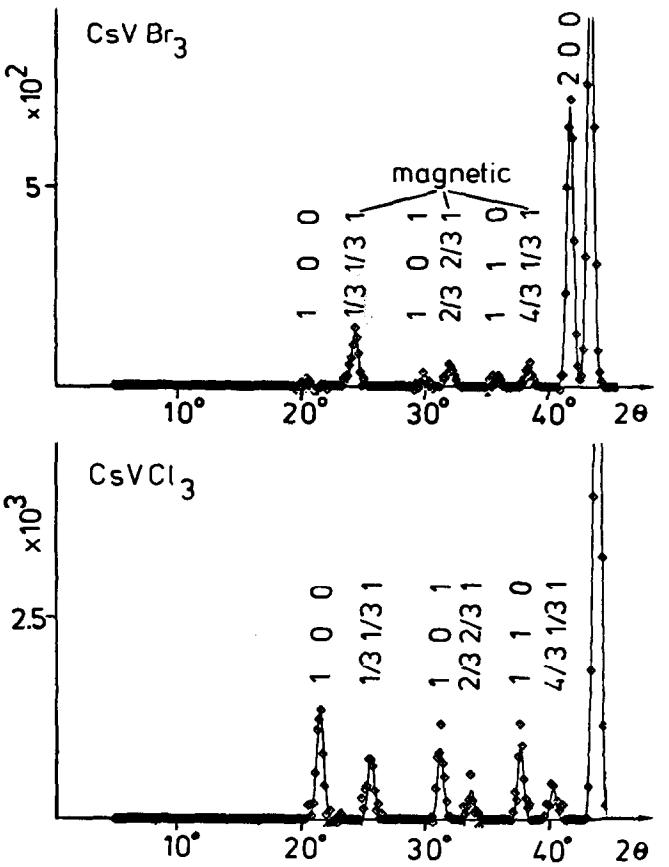

FIG. 4. Diffraction profiles of $CsVBr_3$ and $CsVCl_3$ at 6 K and small scattering angles. $\lambda = 2.34$ Å. Magnetic peaks are indicated.

scattering angles in their low-temperature (6 K) diffraction patterns. This is illustrated in Fig. 4 for $CsVCl_3$ and $CsVBr_3$. The new reflections are of magnetic origin, the magnetic unit cell dimensions being $\sqrt{3}a$, $\sqrt{3}a$, c (referred to the nuclear cell), with 6 V^{2+} ions per magnetic unit cell. For TMVC no peaks of magnetic origin were observed above 1.5 K.

We performed a detailed analysis of the magnetic peaks on a single crystal of $RbVBr_3$ at 4.2 K. In Table IV the experimental intensities for those peaks normalized to the intensity of the $\frac{1}{3}\ \frac{1}{3}\ 1$ reflection are listed. Magnetic intensities are considerably weaker than nuclear intensities, so

TABLE IV

EXPERIMENTAL AND CALCULATED INTEGRATED INTENSITIES OF THE MAGNETIC REFLECTIONS OF $RbVBr_3$ AT 8 K NORMALIZED TO THE $\frac{1}{3}\ \frac{1}{3}\ 1$ REFLECTION (MODEL I: I^{I}_{calc}, MODEL II: I^{II}_{calc})

$h\ k\ l$	I^{magn}_{obs}	I^{I}_{calc}	I^{II}_{calc}
$\frac{1}{3}\ \frac{1}{3}\ 1$	1.000(13)	1.	1.
$\frac{2}{3}\ \frac{2}{3}\ 1$	0.357(13)	0.335	0.439
1 1 1	0.	0.	0.
$\frac{4}{3}\ \frac{4}{3}\ 1$	0.079(5)	0.075	0.129
$\frac{5}{3}\ \frac{5}{3}\ 1$	0.045(3)	0.039	0.079
2 2 1	0.	0.	0.
$\frac{1}{3}\ \frac{1}{3}\ 1$	0.230(17)	0.196	0.347
$\frac{5}{3}\ \frac{5}{3}\ 1$	0.123(14)	0.098	0.188
$\frac{7}{3}\ \frac{1}{3}\ 1$	0.087(10)	0.059	0.133
R^{magn}_{I}		6.3%	20%

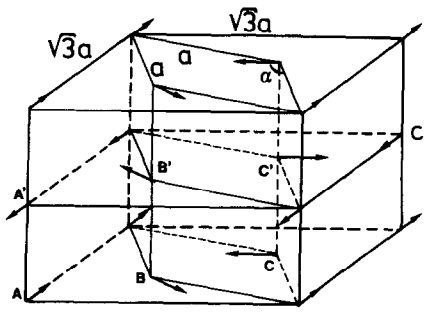

FIG. 5. Magnetic unit cell and spin structure of AVX_3 compounds according to Model I.

effects due to extinction may be ignored. The selection rule l = odd confirms the expected antiferromagnetic order along the c-axis. The second experimental selection rule $h \neq n$ and $k \neq n$ (n a whole number) restricts the possible spin structures still further: the sum of the three spins in the hexagonal planes must be zero. Assuming the ordered magnetic moment per V^{2+} to be equal for all three, the ordered spins must be confined to a plane and form a 120° arrangement. We examine the following special cases for this spin structure: the spins lie in the basal plane perpendicular to the c-axis (Model I) or in the ac-plane (Model II).

In Table IV the calculated intensities for the magnetic diffraction peaks again normalized to the $\frac{1}{3}\,\frac{1}{3}\,1$ reflection for the two models are given. From R_I^{magn} it follows that for $RbVBr_3$ the spin structure of Model I, shown explicitly in Fig. 5, is the more probable. The angle α cannot be determined. The powder data at 6 K of all the other compounds, i.e., $CsVCl_3$, $CsVBr_3$, and $RbVCl_3$, as well as $RbVBr_3$ were refined with the Rietveld program including the magnetic structure of Models I and II. In Table V the R_I^{magn} values for the magnetic fit are given, showing that the magnetic structure of Model I gives a reasonable fit to the experimental data. The spin arrangement of Model I is often encountered in AMX_3 compounds, and is the one expected for an interchain interaction J' of the exchange type (*27*).

In Fig. 6 the temperature dependence of the $\frac{1}{3}\,\frac{1}{3}\,1$ peak for the various compounds is shown, from which we deduced the transition temperatures T_c listed in Table V. The tails of magnetic intensity persisting up to temperatures slightly above T_c indicate some short-range interchain spin correlation. At the same time the lines broaden out quickly. Figure 7 shows the temperature

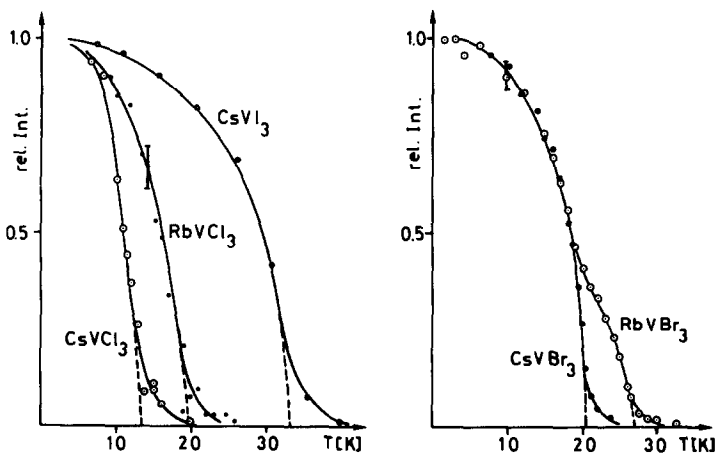

FIG. 6. Temperature dependence of the $\frac{1}{3}\,\frac{1}{3}\,1$ integrated magnetic intensity. Single-crystal data except for $RbVCl_3$.

TABLE V

ORDERING TEMPERATURES T_c, ORDERED MAGNETIC MOMENT μ PER V^{2+} (FROM POWDER DATA), EXCHANGE PARAMETERS J AND J'/J AND R_I^{magn} FOR MODELS I AND II (FROM POWDER DATA, EXCEPT FOR $RbVBr_3$)

	T_c [K]	μ [μ_B]	$2J^b$ [cm^{-1}]	J'/J	R_I^{magn}(I)	R_I^{magn}(II)
$CsVCl_3$	13.8	1.97(7)	−160	2×10^{-4}	0.21	0.36
$CsVBr_3$	20.4	1.87(7)	−(110..120)	1×10^{-3}	0.16	0.60
$CsVI_3$	34.8	1.64(5)[a]	−(25...95)	9×10^{-3}	0.20[a]	0.25
$RbVCl_3$	19(1)	2.31(9)	−180	3×10^{-4}	0.21	
$RbVBr_3$	28.0	1.53(9)	−130[c]	2×10^{-3}	0.06	0.20
$RbVI_3$[a]	25(1)	1.44(6)			0.20	0.32
TMVC	<1.7	—	>−85	$<10^{-4}$		

[a] Ref. (*4*).
[b] Ref. (*5*).
[c] Ref. (*32*).

dependence of the $\frac{1}{3}\frac{1}{3}1$ magnetic reflection for $CsVCl_3$ below 4.2 K. We cannot confirm the decrease in magnetic intensity between 4.2 and 1.3 K reported by Hirakawa *et al.* (*7*). Hirakawa's interpretation of his results in terms of a spin-paired ground state at sufficiently low temperatures instead of a Neel ground state must therefore be treated with caution. Furthermore Feile *et al.* (*24*) could interpret their inelastic neutron scattering results on $CsVCl_3$, $CsVBr_3$, and $CsVI_3$ on the basis of straightforward spin wave theory. A further point to note is the bend at 20 K in the curve for $RbVBr_3$. This indicates that the transition from the 3D ordered phase to the phase with only 1D spin correlation does not take place in one step, but involves an intermediate ordered phase. Whether this phase is incommensurate as observed in a number of AMX_3 compounds such as $RbFeCl_3$ (*25*) or commensurate as in $CsNiCl_3$ (*26*), or whether it is due to the slightly lower nuclear symmetry of $RbVBr_3$ cannot be decided on the basis of the present experimental data. Another indication that things are more complex than it appears at first sight, is the anomalous point at 28 K in the *ac*-susceptibility of $CsVBr_3$ mentioned in the introduction (*6*). The transition temperature T_c from neutron scattering at 20.4 K does not coincide with it.

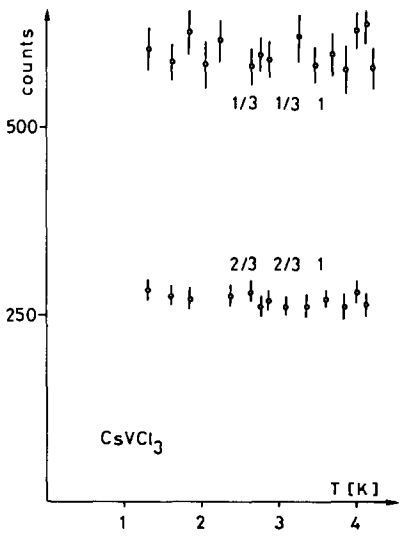

FIG. 7. Temperature dependence of the $\frac{1}{3}\frac{1}{3}1$ and $\frac{2}{3}\frac{2}{3}1$ magnetic intensities for $CsVCl_3$ between 1.3 and 4.2 K.

The intrachain exchange parameters estimated from the magnetic susceptibility measurements by Niel (*5*) and the transition temperatures T_c determined in this study enable us to estimate the J'/J ratio, i.e., the inter- to intrachain interaction (*28*), given in Table V. J'/J is a measure for the 1D character. It increases by almost two

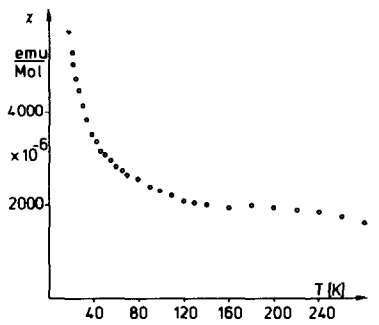

FIG. 8. Temperature dependence of the static magnetic susceptibility of TMVC, $H = 10.32$ kG.

orders of magnitude in the series $CsVCl_3$, $CsVBr_3$, $CsVI_3$, the 1D character therefore decreases strongly. This is supported by the observation of magnetic elastic scattering in $CsVCl_3$ in h k 1 reciprocal lattice planes (*10*) up to room temperature corresponding to a large 1D spin correlation length whereas in $CsVI_3$ no such scattering was found.

The ordered magnetic moments derived from the neutron powder diffraction profiles (see Table V) are reduced up to 50% compared to the magnetic moment of $3\mu_B$ of an isolated vanadium(II) ion in a similar crystal environment (*29*). The two main physical effects which can contribute to such a reduction are:

(i) Zero point fluctuations. Hirakawa *et al.* (*30*) have performed a calculation for the spin reduction ΔS due to zero point fluctuations in quasi-1D triangular antiferromagnets on the basis of first-order spin wave theory. Using their theoretical results and the parameters J and J' listed in Table V, the calculated values for ΔS are 0.95, 0.78, and 0.56 resulting in a calculated ordered magnetic moment of 1.1, 1.4, and 1.9 μ_B for $CsVCl_3$, $CsVBr_3$, and $CsVI_3$, respectively, i.e., a decreasing spin reduction with increasing J'/J ratio.

(ii) Covalency. As a result of covalency some spin density is transferred to the ligands. The trend, in this case, should be opposite, i.e., with increasing covalency from chloride to bromide to iodide the spin reduction should become larger. From the experimental values of the ordered magnetic moment it becomes evident that both effects are of importance. Although the first-order spin wave calculation overestimates the spin reduction, zero point motion can explain the large reductions of μ, but the decrease in the series $CsVCl_3$, $CsVBr_3$, $CsVI_3$ indicates that covalency is at least partly responsible for the observed differences.

In Fig. 8 the magnetic powder susceptibility of TMVC is shown. Below 20 K paramagnetic impurities are predominant (V^{2+} oxidizes very easily to V^{3+}) making a quantitative analysis of the susceptibility curve impossible. But at higher temperatures it shows the typical behavior of a 1D antiferromagnetic chain with large intrachain exchange interaction. From the fact that it starts dropping again above 200 K, an upper limit for the intrachain interaction $-2J$ of 85 cm^{-1} can be estimated. It is not surprising that the intrachain exchange interaction decreases more markedly between $CsVCl_3$ and TMVC than between $RbVCl_3$ and $CsVCl_3$, because the changes both in V–Cl bond distances (superexchange pathway) and V–V distances (direct exchange) are larger in the first case.

In TMVC no additional reflections of magnetic origin were found above 1.7 K, strongly suggesting that TMVC only orders three-dimensionally below this temperature. This means that the J'/J ratio is smaller than 10^{-4}, coming into the same order of magnitude as for $[(CH_3)_4\ N]MnCl_3$ (TMMC) (*31*). Although the intrachain interaction in TMVC is smaller than in $RbVCl_3$ and $CsVCl_3$, its 1D character seems to be more pronounced, i.e., the interchain interaction must be very much smaller in TMVC. In TMVC the chains are much better separated by the bulky $(CD_3)_4\ N^+$ ions than by Rb^+ and Cs^+ in $RbVCl_3$ and

$CsVCl_3$, the intrachain separation of V^{2+} ions being 2.13 and 1.93 Å, respectively, smaller than in TMVC.

Acknowledgments

We thank Mr. K. Mattenberger of the ETHZ for the susceptibility measurements on TMVC. Part of this work was supported by the Swiss National Science Foundation (Grant 2.673.080).

References

1. H. J. SEIFERT AND B. KIEWISCH, *J. Therm. Anal.* **13,** 33 (1978).
2. H. J. SEIFERT AND P. EHRLICH, *Z. Anorg. Allg. Chem.* **30,** 282 (1959).
3. M. NIEL, dissertation, Bordeaux 1976.
4. H. W. ZANDBERGEN, *J. Solid State Chem.* **37,** 308 (1981).
5. M. NIEL, C. CROS, M. POUCHARD, AND J.-P. CHAMINADE, *J. Solid State Chem.* **20,** 1 (1977).
6. A. J. VAN DUYNEVELDT, private communication.
7. K. HIRAKAWA, H. YOSHIZAWA, AND K. UBUKOSHI, *J. Phys. Soc. Jpn.* **51,** 1119 (1982).
8. A. HAUSER, U. FALK, P. FISCHER, A. FURRER, AND H. U. GÜDEL, *J. Magn. Magn. Mater.* **31-4,** 1139 (1983).
9. P. W. ANDERSON, *Mater. Res. Bull.* **8,** 153 (1973).
10. M. STEINER, J. M. DANCE, AND M. NIEL, "Berichte aus der Arbeitsgruppe Neutronenstreuung," HMI-B 332 (1980).
11. A. HAUSER AND H. U. GÜDEL, *Chem. Phys. Lett.* **82,** 72 (1981).
12. A. HAUSER AND H. U. GÜDEL, *J. Magn. Magn. Mater.* **31-4,** 1239 (1983).
13. W. E. SMITH, *J. Chem. Soc. Dalton,* 1634, 1972.
14. G. L. MCPHERSON, A. M. MCPHERSON, AND J. L. ATWOOD, *J. Phys. Chem. Sol.* **41,** 495 (1980).
15. H. J. SEIFERT, H. FINK, AND E. JUST, *Naturwissenschaften* **55,** 297 (1968).
16. H. J. SEIFERT AND T. AUEL, *Z. Anorg. Allg. Chem.* **360,** 50 (1968).
17. H. M. RIETVELD, *J. Appl. Crystallogr.* **2,** 65 (1969).
18. Newsletter of the Neutron Diffraction Commission, 1982.
19. R. E. WATSON AND A. J. FREEMAN, *Acta Crystallogr.* **14,** 27 (1961).
20. G. D. STUCKY, S. D'AGOSTINO, AND G. L. MCPHERSON, *J. Amer. Chem. Soc.* **88,** 4828 (1966).
21. "Handbook of Chemistry and Physics," 59th ed., F-215, CRC Press, Boca Raton, Fla. (1978).
22. CH. BAUERHOFER, "The X-Ray Rietveld System," Institut für Kristallographie, ETHZ.
23. B. MOROSIN AND E. J. GRAEBER, *Acta Crystallogr.* **23,** 766 (1967).
24. R. FEILE, J. K. KJEMS, A. HAUSER, H. U. GÜDEL, U. FALK, AND A. FURRER, *Solid State Commun.* **50,** 435 (1984).
25. N. WADA, K. UBUKOSHI, AND K. HIRAKAWA, *J. Phys. Soc. Jpn.* **51,** 2833 (1982).
26. W. B. YELON AND D. E. COX, *Phys. Rev. B* **7,** 2024 (1973).
27. M. STEINER, J. VILLAIN, AND G. G. WINDSOR, *Adv. Phys.* **25,** 87 (1976).
28. H. J. HENNESSY, C. D. MCELWEE, AND P. M. RICHARDS, *Phys. Rev. B* **7,** 930 (1973).
29. G. L. MCPHERSON, T. J. KISTENMACHER, AND G. D. STUCKY, *J. Chem. Phys.* **52,** 815 (1970).
30. H. KADOWAKI, K. HIRAKAWA, AND K. UBUKOSHI, *J. Phys. Soc. Jpn.* **52,** 1799 (1983).
31. L. J. DE JONGH AND A. R. MIEDEMA, "Experiments on Simple Magnetic Model Systems," p. 38, Taylor & Francis, London (1974).
32. U. FALK, unpublished results.